Master I research project

course: Phys-F436

Interuniversity Institute for High Energies

Resolution limits of Icecube on the detection of neutrinos emitted by the evaporation of primordial black holes

Author:
Ibrahim Khaled

Supervisor:
Prof. Juan A. Aguilar Sánchez

September 3, 2018

Abstract

Primordial black holes are hypothetical black holes formed in the early universe. As all black holes, they can emit particles like gamma or neutrinos by mean of the evaporation mechanism. To show their existence, it would be wise to detect neutrinos emitted by them. In this work, we determined by means of IceCube data whether we were able to detect events that could potentially be a neutrino emission from PBHs. We saw three clusters in the north of the sky map and each of them show two events. We calculated the approximate point source flux equivalent to these two events and set a limit for further possible detection.

Contents

1 Introduction **2**

2 IceCube Detector **3**
2.1 Overview 3
2.2 Experimental mechanism and search strategies 4
2.3 Data samples 7

3 Detection method and results **8**
3.1 Time Dependent likelihood method 8
3.2 All-Sky Time Scan 9
3.3 Results 10

4 Conclusion **15**

A The code **16**

B Tables **18**

Chapter 1

Introduction

Our universe is incredibly complex and still hides so many mysteries such as black holes. It is known that black holes are formed at the end of the life of a massive star after the core-collapse supernovae. But there might exist another type of black hole whose origin could be different. Those hypothetical black holes could have been formed at an earlier time, in the first moments of the universe, they are usually referred to as primordial black holes. According to [4] they can be formed by the collapse of the universe density fluctuations which can occur during a cosmic phase transition [8] or during more exotic mechanisms. Their existence was first suggested by Yakov Borisovich Zel'dovich and Igor Dmitriyevich Novikov in 1966 [12] but it is Stephen Hawking who first studied the theory behind their origins. In 1975, Hawking showed that black holes can release radiation due to quantum effect near the event horizon [7]. The so called Hawking radiation looks like a black body spectrum with temperature inversely proportional to the black hole mass. Therefore, primordial black holes have a low mass compared to stellar ones because only black holes with a mass below $M_* \simeq 4 - 6 \times 10^{14} g$ evaporate within the age of the Universe through this mechanism. A black hole can emit particles with energy in the range (E,E+dE) at a rate of

$$\frac{d^2N}{dtdE} = \frac{1}{2\pi\hbar} \frac{\Gamma_s(E, M)}{\exp(8\pi GME/\hbar c^3) - (-1)^{2s}} \tag{1.1}$$

Here M is the mass of the black hole, s the particle spin and Γ_s the absorption coefficient. For more details see [5]. Thus the direct neutrino flux is given by equation 1.1 and it is the same for all neutrino flavors. On the contrary, indirect flux is flavor dependent and split into two categories. One can be the decay products of directly emitted heavier particles: $\mu^{\pm} \to \bar{\nu}_{\mu}(\nu_{\mu})\nu_e(\bar{\nu}_e)e^{\pm}$ or $\tau \to e\bar{\nu}_e\nu_{\tau}/\tau \to \mu\bar{\nu}_{\mu}\nu_{\tau}$. The second case is when we exceed QCD deconfinement temperature, the flux can be produce by the decay of quark and gluon fragmentation products: $\pi^{\pm} \to \mu^{\pm}\nu_{\mu}(\bar{\mu_{\nu}})$ As it was done in [5], we make the approximation that all the fragmentation products are pions. In this article, they calculated the accumulated diffuse flux of all PBHs which evaporated within the lifetime of our Universe. It was done for a PBH density taken to be the maximum allowed by bounds derived from gamma ray measurements [6]. They find some characteristics as E^{-3} decreases at high energies with a "knee" in a certain range of energy. But all of these observations were theoretical in the case of diffuse flux. What flux can we obtain if we search for a point source ? Can we detect neutrino coming from this type of source ? Using data from large detector like IceCube, we will try to answer these questions.

Chapter 2

IceCube Detector

2.1 Overview

Figure 2.1: The IceCube Lab - 2013 Credit: Felipe Pedreros, IceCube/NSF

2010 marks the end of the construction of the IceCube Neutrino Observatory, a huge detector of high energy neutrinos in Antarctica near the south Pole. Its main goal is to detect neutrinos from astrophysical origin, induced by cosmic rays or atmospheric muons. The IceCube detector consists of an array of 5160 Digital Optical Modules (DOMs) placed deep into the ice. These spherical optical sensors are made of pressure resistant glass housing, each of them containing a photomultiplier tube (PMT) and the associated electronics for data acquisition. As it is shown in the figure 2.2, these DOMs are connected together in 86 vertical strings of 60 DOMs each.

Each string was placed into 60 cm wide holes drilled into the ice using hot water to form a kilometer cubed volume in a depth range going from 1.5 km to 2.5 km.

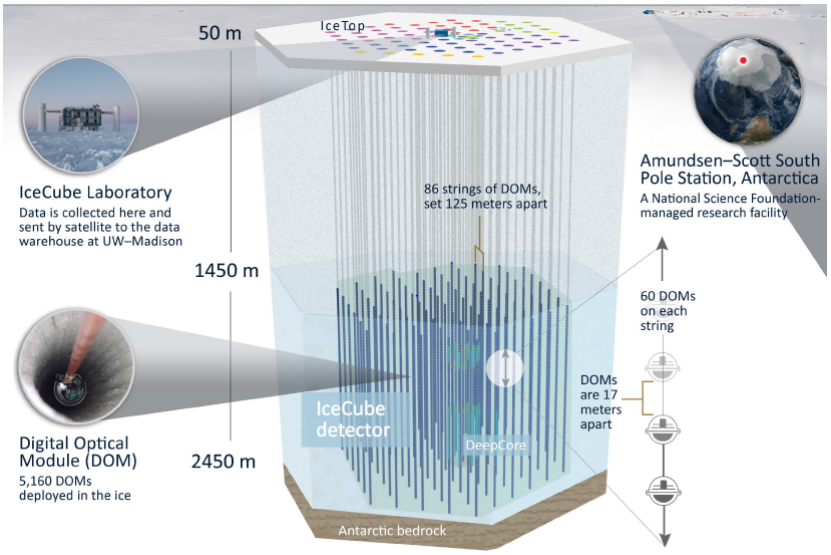

Figure 2.2: This figure from the icecube website represents the IceCube Neutrino Observatory with all of its detectors.

The IceCube is also composed of several sub-detector in addition to the main one: AMANDA, IceTop and the Deep Core.

- AMANDA: the Antarctic Muon And Neutrino Detector Array was the first piece of the IceCube project. It was used as a proof of concept to demonstrate that the extremely clear Antarctic ice was suitable for detecting energetic neutrinos. This first detector was turned off in 2009.
- IceTop: it is a series of detectors composed of 81 stations located on top of each IceCube's strings. This surface array measures the cosmic-ray arrival directions in the Southern Hemisphere as well as the flux and composition of cosmic rays. This allows us to use IceTop as a veto and a calibration detector for IceCube and it is also used to detect air showers from primary cosmic rays in the 300 TeV to 1 MeV energy range.
- Deep Core: it is a sub-array formed by strings placed next to each other in the center of the detector. Its disposition enhances the sensitivity of the detector and allows to detect neutrinos with energies below the standard IceCube threshold of 100 GeV.

2.2 Experimental mechanism and search strategies

IceCube is what we call a Cherenkov detector because it uses the Cherenkov radiation to detect particles. When relativistic charged particles, like leptons emitted during neutrinos interactions, go through a medium where its speed is greater than the speed of light in that medium, it can induce a radiation that we call the Cherenkov radiation. Cherenkov light produced by the particle is emitted in the UV and blue region in a narrow cone with an angle such that

$$\cos\theta = 1/\beta n$$

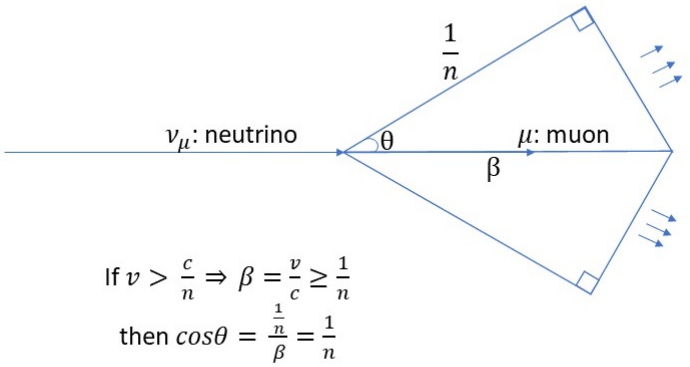

Figure 2.3: This figure represents the Cherenkov effect when a relativistic charged particle goes through a medium where its speed is greater than the speed of light in that medium

where n is the index of the medium and $\beta = v/c$ the Lorentz factor.

Thanks to the Cherenkov radiation, the detector can indirectly detect those neutrinos. Light is first collected by photomultiplier tubes which are vacuum tubes consisting of input window where light passes through. Then, it excites the electrons in the photo-cathodes and photoelectrons are emitted. They are accelerated and focused onto the first dynode where they are multiplied by mean of secondary electrons emission. The multiplied secondary electrons emitted from the last dynode are collected by the anode and produce an output signal. More details about the principles of photomultiplier tubes can be found in [9].

By means of this process, we can get light patterns that reveal the direction and the energy of muons and neutrinos. We can see in ice two different signatures:

- Track topology: Good angular resolution 0.1°-1° but detect only one flavor of neutrino (ν_μ).
- Cascade topology: Detect all flavors, calorimeter are fully active so it provides a good energy resolution.

There is a lot of background signal from muon that are created when cosmic ray hit the atmosphere above the detector. Therefore, keys to discriminate this background signal are direction and energy.

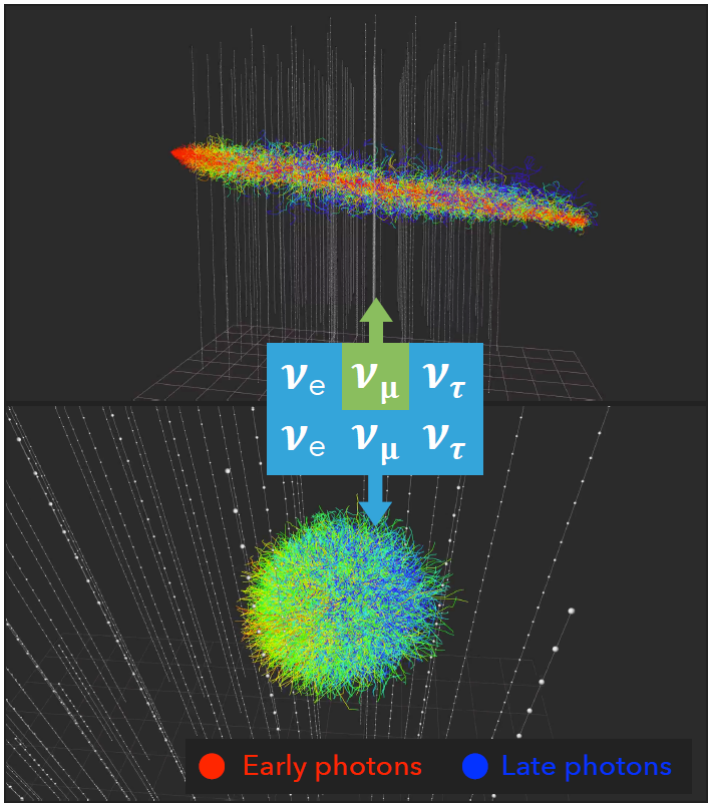

Figure 2.4: Signatures in ice (this image comes from the astroparticle Physics course 2018 of Professor J.Juan Aguilar Sánchez

Icecube uses two kinds of search strategies:

- Diffuse: If sources are numerous but faint, it uses energy as the key to discriminate astrophysics neutrinos from background noise. We can thus make the distinction between two sources. Icecube can use Earth as a shield against atmospheric muons to detect up-going through-going muon events. It can also use the outer layers (see figure 2.5) as an active veto to select starting events. Researchers from Icecube collaboration have found after collecting 6 years of data, a signal with 5.9σ using the first technique and with 4 years of data a 6.5σ for the second technique(TeVPA 2015, Tokyo).

- Point-Sources: In contrast to the diffuse strategy, if sources are few but bright, we use both energy from up and down going muons and directional information to identify clustering of neutrinos in a given direction. Notice that up and down going muons have different origins, the first are mostly produced by interaction of atmospheric neutrinos with earth when they pass through and the second from pions and mesons decays during atmospheric showers caused by cosmic rays. Thus, atmospheric muons and neutrinos are considered as background noise. Using the data collected during 6 years, we still have no significant excess over background signal [1]. In this case, we set an upper limit in terms of energy or flux of neutrinos which allows us to know where we will not see any signal.

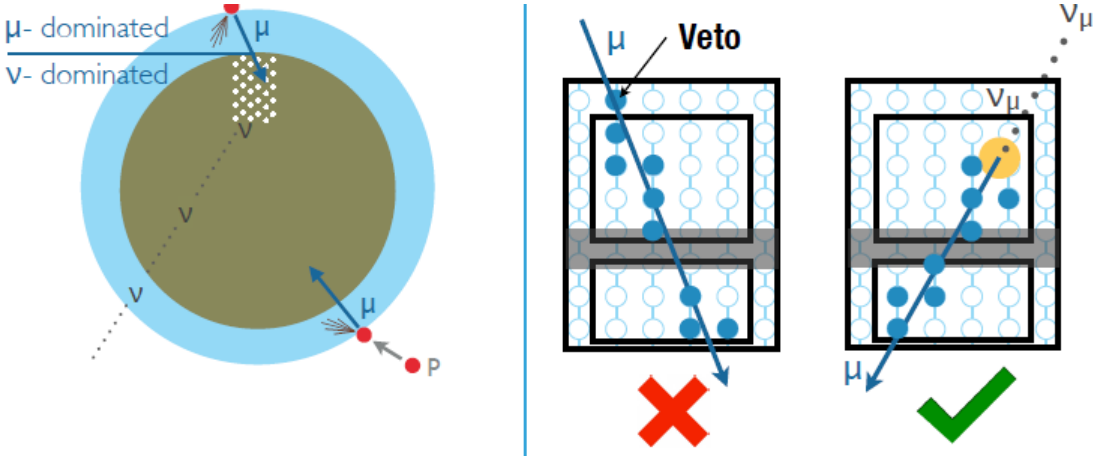

Figure 2.5: This figure comes from the astroparticle Physics course 2018 of Professor J.Juan Aguilar Sánchez show the diffuses search strategy

Indeed, we can already point out that we are in this last strategy case for a data collecting method, knowing that our goal is to detect neutrinos from primordial black holes which is an astrophysical source of neutrinos.

2.3 Data samples

The IceCube detector took data even before its full completion. This is the reason we have some data before 2010. Among all the data samples available since 2008 to 2012, we will only use the sample IC-86I which corresponds to data taken during one year (2011 May 13 to 2012 May 16) when all strings were operational.

sample	start (MJD)	end (MJD)	livetime [days]	atm. νs/day	up-going	down-going
IC-40	2008 Apr 5 (54561)	2009 May 20 (54971)	376	40	14121	22779
IC-59	2009 May 20 (54971)	2010 May 31 (55347)	348	120	43339	64230
IC-79	2010 May 31 (55347)	2011 May 13 (55694)	316	180	50857	59009
IC-86I	2011 May 13 (55694)	2012 May 16 (56063)	333	210	69227	69095

Figure 2.6: Summary of the data used in the article [10]. Where MJD is the abbreviation of modified Julian days

In this work, we will look at this data to see if IceCube could detect a signal that could correspond to neutrinos coming from a primordial black hole. In the next chapter, we will describe the method we used to analyze the data and extract information.

Chapter 3

Detection method and results

The data were collected over a period of one year during which the sky was scanned for a point source accumulation which would be a potential signal or just a fluctuation of the background noise. Considering the background noise as constant over time, the source of the signal depends on the time. We are therefore looking for a point source that depends on time.

3.1 Time Dependent likelihood method

In our analysis, we will use the Time dependent likelihood method which has been applied in previous analysis (source). Let us first describe mathematically what is the signal of the background noise and of the point source. We define $B(\delta, E, t)$ as the background noise probability density function, which depends on declination δ (space dependence), energy and time. B can be estimated from the data itself and has the form :

$$B_i = P_i^b(\delta_i)\epsilon_i^b(E_i, \delta_i)T_i^b \tag{3.1}$$

Where each event i belongs to the sample IC-86I, P_i is the spatial part of the background noise, ϵ_i the energy probability density function and T_i the time PDF (probability density function). P_i depends only on the declination because for sufficiently long time scales, it is uniform in right ascension as the Earth rotation averages over detector effects. T_i is uniform as the seasonal variations of background atmospheric μ and ν_μ are negligible compared to possible signals [11].

The signal probability density function is given by:

$$S_i = P_i^s(|\vec{x_i} - \vec{x_s}|, \theta_i)\epsilon^s(E_i, \delta_i)T_i^s \tag{3.2}$$

where $\vec{x_s}$ is the source direction, $\vec{x_i}$ the reconstructed direction of the event, θ_i the angular error estimate for the reconstruction and E_i and δ_i the energy and declination respectively. Here the time probability function is different for each hypothesis on the signals. As [10] we decided to use Gaussian function as parametrization which is generally used for a limited duration increase in the emission of a source.

$$T_i^s = \frac{1}{\sqrt{2\pi\sigma_T}} \exp\left(-\frac{(t_i - T_0)^2}{2\sigma_T^2}\right) \tag{3.3}$$

where t_i is the arrival time of the i^{th} event and naturally T_0 is the mean and σ_T the width of the Gaussian.

Now we define the likelihood function as :

$$L(\gamma, n_s, ...) = \prod_i n_s S_i + (1 - n_s) B_i \tag{3.4}$$

with n_s the number of signal event and γ the spectral index from $dN/dE \propto E^{-\gamma}$ and is assumed to be the same for all data samples. In subsection 3.3, we will set it to the value of two because we want to find the flux corresponding to our $\hat{n}_s$ value.

3.2 All-Sky Time Scan

The all sky time scan is the most generic time dependent search. It is used to look at neutrino emission from a punctual source with limited duration which is perfectly adapted for our study. For this search the whole sky was divided into grid of $0.1° \times 0.1°$ whose size is better than the angular resolution of the detector. Thus a single point is not significant, we must take into account all the correlated points to deduce the potential location of a flair. The maximization of the likelihood function allows us to find the best parameters ($\hat{n}_s$, $\hat{\gamma}$, $\hat{\sigma}_T$ and $\hat{T}_0$) for each grid points.

We have two different hypotheses:

- The null hypothesis H_0 when no signal is detected. This corresponds to a likelihood where $n_s = 0$ thus $L(n_s = 0) = B_i$
- The signal-plus-background hypothesis H_1 when the likelihood is evaluated with the best parameters $\hat{\gamma}, \hat{n}_s, \hat{\sigma}_T, \hat{T}_0$. to have a signal.

We are going to test which one of those hypotheses is true using the Test Statistic TS described in [10].

$$TS = -2 \log \left[\frac{T}{\sqrt{2\pi\hat{\sigma_T}}} \frac{L(H_0)}{L(H1)} \right] \tag{3.5}$$

By maximizing the likelihood at each grid point in the sky, we get TS values that serve as an estimate of local significant of the best fit parameters and we obtain maps as in the figure below.

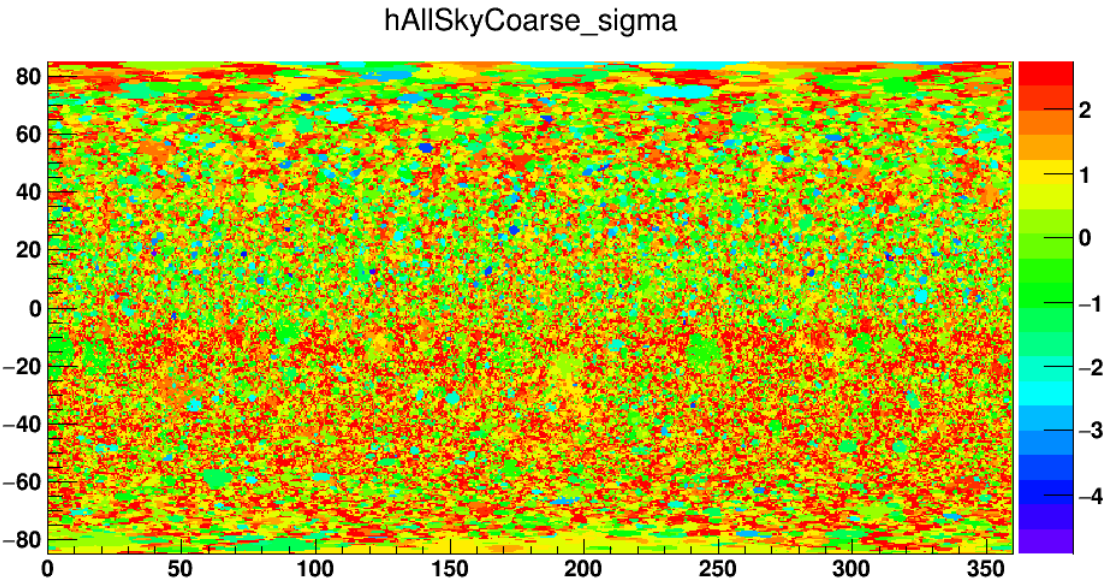

Figure 3.1: This is a map of $\log_{10} \hat{\sigma_T}$ in color graduation. On the horizontal axis we have the right ascension and vertical axis is the declination. Values of $\hat{\sigma_T}$ are obtained by mean of TS.

Using the information behind this, we can localize areas where we have a fluctuation compared to the background noise. To detect neutrino PBH, we want events where

- $\hat{\sigma}_T < 2s$
- $2 < \hat{\sigma}_T < 3s$
- $3s < \hat{\sigma}_T < 4s$
- $4s < \hat{\sigma}_T < 5s$

Indeed, the burst is coming from hadronic process or hardonic models suggest production of neutrinos and γ-rays from pion decays thus there is a strong correlation between the two type of bursts coming from the PBH [3].

We are looking at the position of points where the criteria above are satisfied. Using those positions we look at the corresponding values of others likelihood parameters and extract information. This was performed with a macro in ROOT which recovers the data obtained and saved it in a file. The code can be found in the annex.

3.3 Results

First of all, we notice by looking at the data that we have only one single point that follows the criteria two. Thus, we decided to exclude it because a single point is not relevant. By means of the position data, we can identify three clusters on the skymap as you can see on the figure 3.2. The green one is at $[19°, 40°]$, the blue at $[91°, 12°]$ and the last red cluster is at $[122°, 13°]$.

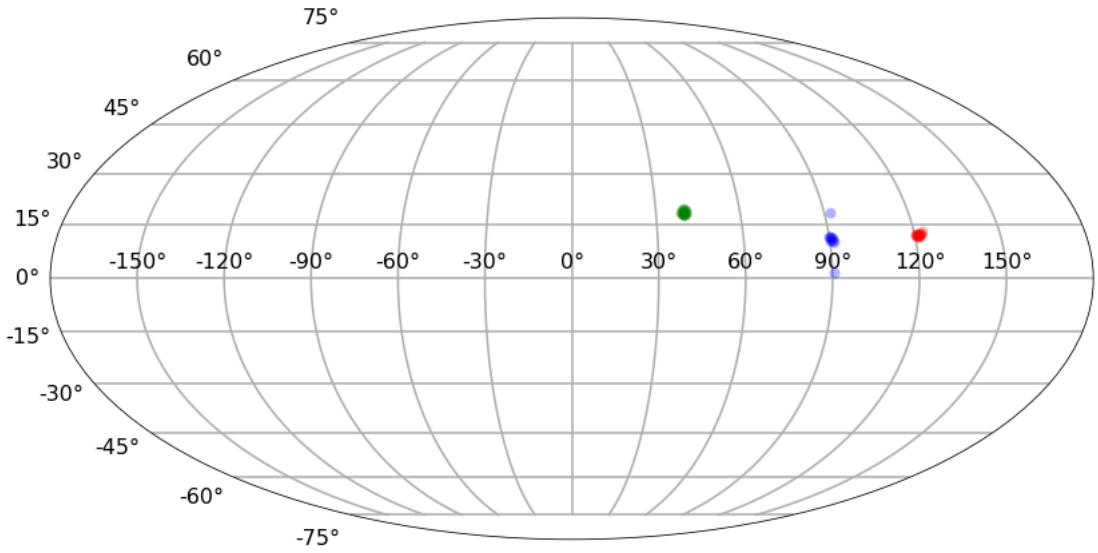

Figure 3.2: The skymap in equatorial coordinates shows three clusters corresponding to fluctuation of the background noise. The green points are data for the first condition, blue for the second and red for the 4^{th}. If we look at the figure 6 on [10] , we can also know the range of p-values for our clusters because this figure shows p-values for the best fit flare hypothesis tested in each direction of the sky.

On figure 3.3, we plotted the number of events with respect to $\hat{\sigma}_T$. We can see that we get three clusters where the number of events is two, which is the minimum required to identify a flare.

On figure 3.4, we can deduce the range of p-values or equivalently $-\log_{10} p$ for our data [0.6;1.7] and it is clearly not significant if we compare to 5σ discovery where $-\log_{10} p \approx 6$.

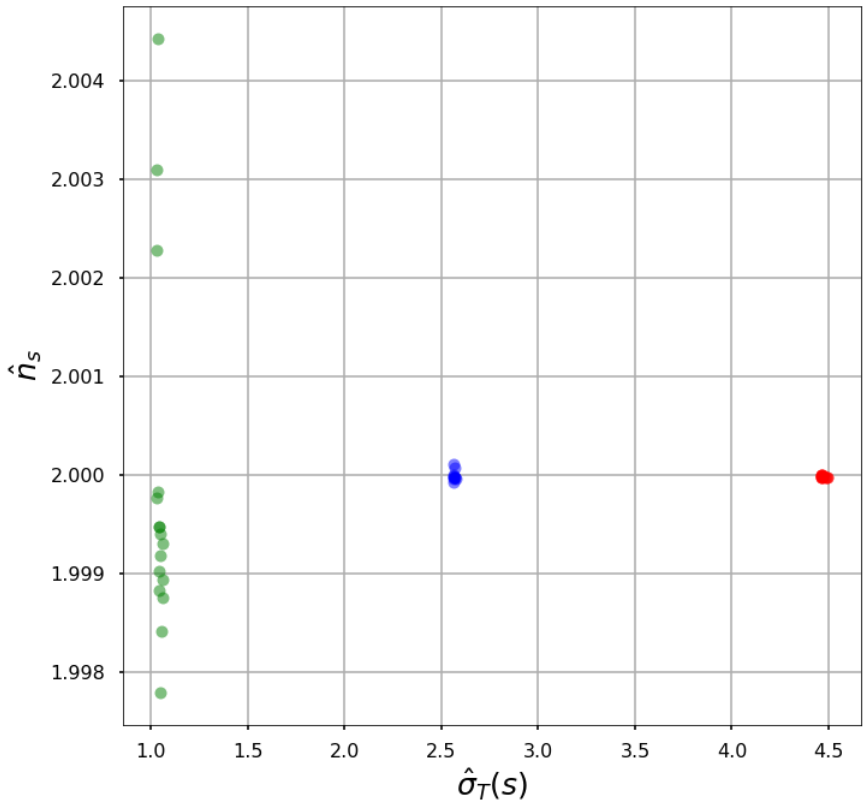

Figure 3.3: Number of events with respect to $\hat{\sigma}_T$ where the green points are data for the first condition, blue for the second and red for the 4^{th}

We want to know which flux corresponds to those two events for the conditions above. The number of observed events is given by:

$$N_{ev} = \int \Phi_0 A_{eff}(E) \Delta t E^{-\gamma} dE \tag{3.6}$$

Where N_{ev} is the number of events Φ_0 is the normalization of an average flux, Δt is $\hat{\sigma}_T$ for each cluster and γ is the spectral index. For our calculation we have assumed that $\gamma = 2$ to have an energy spectrum of the form E^{-2}. We need A_{eff} the Ice Cube effective area given in the plot below from [2]. We are interested by the curve where the declination is between $-5°$ and $30°$ (blue curve) because our clusters are in this area as seen on figure 3.2. To simplify the integral calculation we assume that A_{eff} is constant over different ranges of energy. Thus, we transform the integral into a sum of integrals where A_{eff} has a constant value in each of them. We notice that this is a rough estimation of the equivalent flux because as you can see on figure 3.5, it is difficult to set a range of energy where A_{eff} is really constant.

$$N_{ev} = \Phi_0 \left[\int_{10^{-1}}^{Emax_i} A_{eff} \Delta t E^{-2} dE + ... + \int_{Emin_i}^{10^6} A_{eff} \Delta t E^{-2} dE \right] \tag{3.7}$$

After calculation, we find values regrouped in table 3.1.

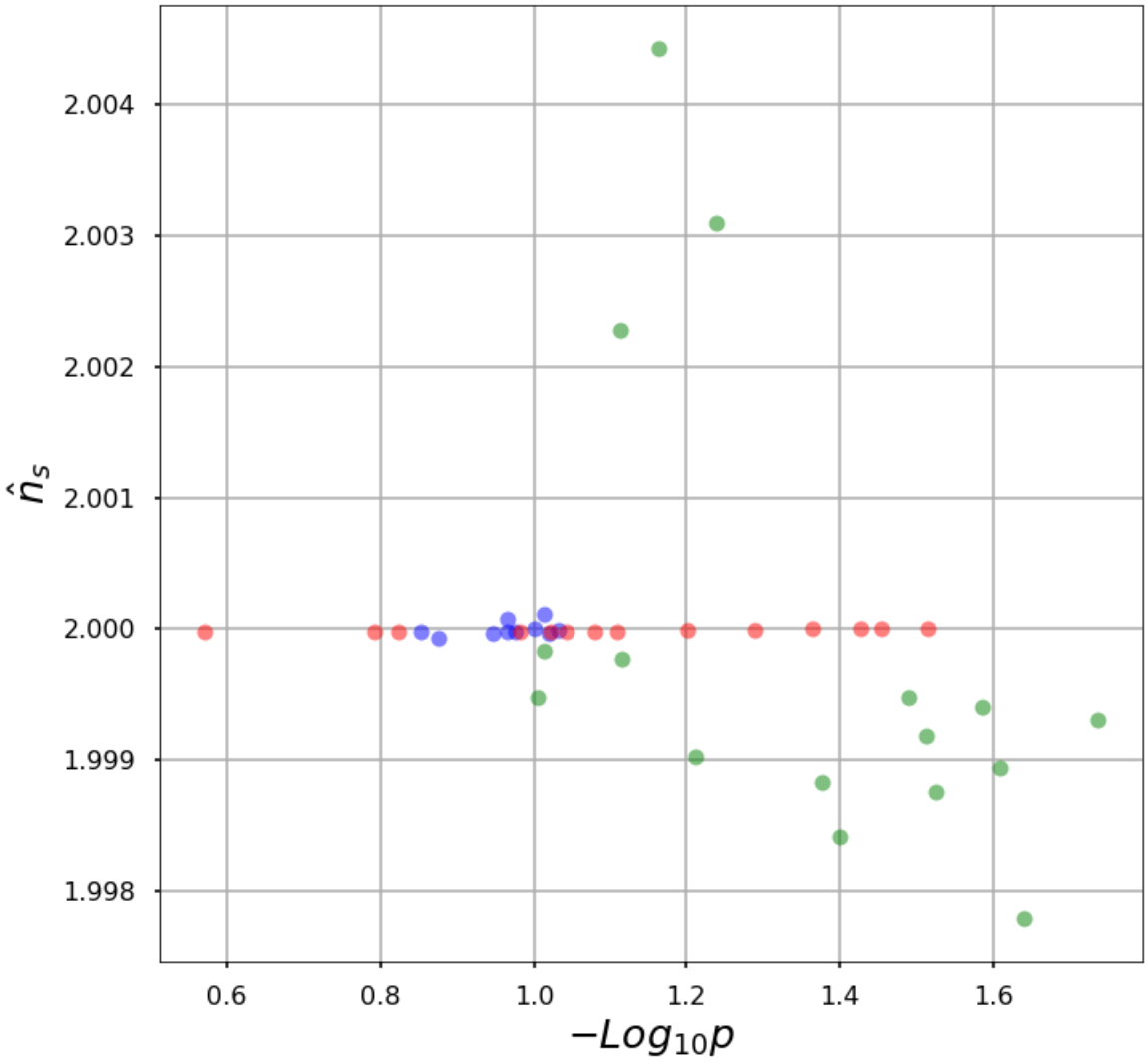

Figure 3.4: The number of events with respect to $-\log_{10} p$ where green points are data for the first condition, blue for the second and red for the 4^{th}

$\hat{\sigma}_T$(s)	$\phi(particle/TeVm^2s)$
1	$0.311915E^{-2}$
2.6	$0.119967E^{-2}$
4.5	$0.0693145E^{-2}$

Table 3.1: Table of the equivalent flux for $\hat{n}_s = 2$ for each cluster

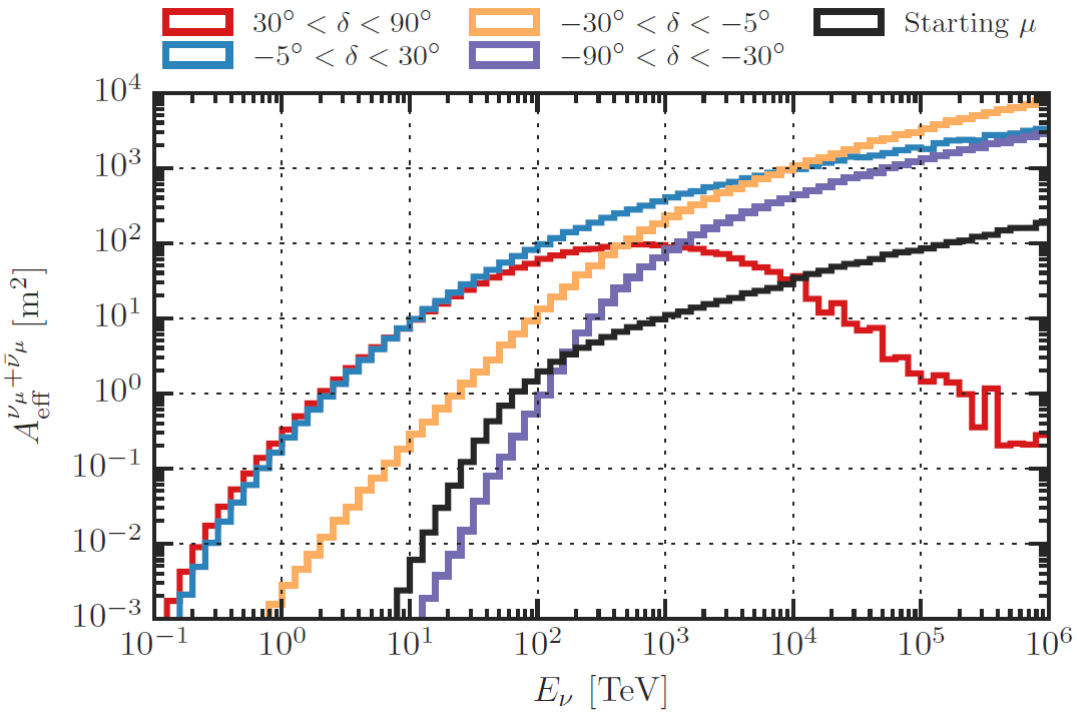

Figure 3.5: IceCube effective area vs neutrino energy [2]

Chapter 4

Conclusion

In this work, we found fluctuations of the background noise corresponding to our criteria but the p-values associated are not large enough to conclude that we have a discovery of PBH. However it doesn't imply that Ice Cube is not capable of detecting such neutrinos. We now know to which flux that number of events corresponds to. This allows us to set an upper-limit on the flux where events with a flux higher than the upper-limit doesn't correspond to PBH neutrinos. Using the flux we found, we could also find the maximum distance for which the alleged PBH is detectable as described in [5]. For further research we could reproduce the same investigation with more data and deduce the flux resulting from it and compare it with our result to get more details about flux characteristics.

Appendix A

The code

```
 {
ofstream fichier("BHNdetection.txt", ios::out | ios::trunc);
//If it's open
if(fichier)
 {
   //Import histograms
   TFile DATA("C:\\root_v5.34.36\\DATA.root");
   TH2D *histo = DATA.Get("hAllSkyCoarse_sigma;1");
   TH2D *histons = DATA.Get("hAllSkyCoarse_ns;1");
   TH2D *histogamma = DATA.Get("hAllSkyCoarse_gamma;1");
   TH2D *histomean = DATA.Get("hAllSkyCoarse_mean;1");
   TH2D *histopvalue = DATA.Get("hAllSkyCoarse;1");
   //histo->Draw("colz");
   //cout << "opened histo with nbins " << histo->GetNbinsX() << endl;
   //Searching the maximum bins on x and y axes
   double nbinx = histo -> GetNbinsX();
   double nbiny = histo -> GetNbinsY();
   //Searching the index where the content of the bins respect the condition
   for (int i = 0; i < nbinx; i++)
   {
     for (int j = 0; j < nbiny; j++)
     {
       Float_t content = histo->GetBinContent(i,j);
       Float_t ns = histons->GetBinContent(i,j);
       Float_t gamma = histogamma->GetBinContent(i,j);
       Float_t mean = histomean->GetBinContent(i,j);
       Float_t pvalue = histopvalue->GetBinContent(i,j);

       //content is the date of the event in julien day and the condition is
       //that content<log(2,3,4 and 5 seconds in Julien days)
        if(content < TMath::Log10(2./24./60./60.))
        {
          double  x = histo->GetXaxis()->GetBinCenter(i);
          double  y = histo->GetYaxis()->GetBinCenter(j);
          fichier << "event with log(sigma)<log(2s in MDJ)"<< endl;
```

```
        fichier <<  "content: "<< content << "\t" << "index i: "<< i <<  "\t"
        <<"index j: "<< j <<  "\t" <<"ascension: "<< x <<  "\t" <<"declination =  "<< y <<"\t
       "\t"<<"Mean : "<< "\t"<< mean<<"\t"<< "p-value (in -log10):"<< pvalue<< endl;
      }
       if(TMath::Log10(2./24./60./60.) <content && content < TMath::Log10(3./24./60./60.))
      {
        double  x = histo->GetXaxis()->GetBinCenter(i);
        double  y = histo->GetYaxis()->GetBinCenter(j);
        fichier << "event with log(2s  in MDJ)<log(sigma)<log(3s in MDJ)" << endl;
        fichier <<  "content: "<< content << "\t" << "index i: "<< i <<  "\t"
        <<"index j: "<< j <<  "\t" <<"ascension: "<< x <<  "\t" <<"declination =  "<< y <<"\t
        "\t"<<"Mean : "<< "\t"<< mean<< "p-value (in -log10):"<< pvalue<< endl;
      }
     if(TMath::Log10(3./24./60./60.) < content && content < TMath::Log10(4./24./60./60.))
       {
         double  x4 = histo->GetXaxis()->GetBinCenter(i);
         double  y4 = histo->GetYaxis()->GetBinCenter(j);
         fichier << "event with log(3s  in MDJ)<log(sigma)<log(4s in MDJ)"<< endl;
         fichier <<  "sigma in log10: "<< content << "\t" << "index i: "<< i <<  "\t"
         <<"index j: "<< j <<  "\t" <<"ascension: "<< x <<  "\t" <<"declination =  "<< y <<"\
         "\t"<<"Mean : "<< "\t"<< mean<< "p-value (in -2log10):"<< pvalue<< endl;
       }

     if(TMath::Log10(4./24./60./60.) < content && content < TMath::Log10(5./24./60./60.))
       {
         double  x = histo->GetXaxis()->GetBinCenter(i);
         double  y = histo->GetYaxis()->GetBinCenter(j);
         fichier << "event with log(4s  in MDJ)<log(sigma)<log(5s in MDJ)" << endl;
         fichier <<  "content: "<< content << "\t" << "index i: "<< i <<  "\t"
         <<"index j: "<< j <<  "\t" <<"ascension: "<< x <<  "\t" <<"declination =  "<< y <<"\
         "\t"<<"Mean : "<< "\t"<< mean<< "p-value (in -log10):"<< pvalue<< endl;
       }
    }
   }
   //we close the file
   fichier.close();
   cout<<"End of writing"<<std::endl;
    }
  //if not
  else
  {
     std::cout <<"Error opening file "<<std::endl;
  }
}
```

Appendix B

Tables

Table B.1: Data for $\hat{\sigma_T} < 2s$

p-value	$\hat{n_s}$	$\hat{T_0}(MJD)$	γ	$\hat{\sigma_T}$(s)	$-\log_{10} p$
0,068617517	2,00442	56744,9	3,94902	1,035914096	1,163565
0,032350426	1,99948	56744,9	3,94876	1,044152043	1,49012
0,0259651	1,9994	56744,9	3,94873	1,045066057	1,58561
0,042072663	1,99883	56744,9	3,94892	1,043358942	1,376
0,057725805	2,00309	56744,9	3,94893	1,028380286	1,23863
0,022892067	1,9978	56744,9	3,94871	1,049841515	1,640315
0,018375747	1,99931	56744,9	3,94944	1,05743515	1,735755
0,029919546	1,99876	56744,9	3,94978	1,061167016	1,524045
0,097072229	1,99983	56744,9	3,94928	1,03372196	1,012905
0,076923671	2,00228	56744,9	3,94995	1,029707183	1,11394
0,030673618	1,99919	56744,9	3,94966	1,049044093	1,513235
0,024575366	1,99894	56744,9	3,94873	1,059604374	1,6095
0,039879986	1,99842	56744,9	3,94967	1,051535024	1,399245
0,076666388	1,99977	56744,9	3,94999	1,030608553	1,115395
0,061535396	1,99903	56744,9	3,94898	1,043022657	1,210875
0,098657476	1,99948	56744,9	3,94907	1,040144657	1,00587

Table B.2: Data for $2s < \hat{\sigma_T} < 3s$

p-value	$\hat{n_s}$	$\hat{T_0}(MJD)$	γ	$\hat{\sigma_T}$(s)	$-\log_{10} p$
0,140165135	1,99998	56857,4	3,9494	2,562381219	0,85336
0,0996185	2	56857,4	3,94915	2,56285327	1,00166
0,097084523	2,00011	56857,4	3,94944	2,560729723	1,01285
0,113150115	1,99997	56857,4	3,94999	2,561850265	0,946345
0,095323504	1,99996	56857,4	3,94931	2,572549514	1,0208
0,092909474	1,99999	56857,4	3,94921	2,562971297	1,03194
0,108322831	1,99998	56857,4	3,94976	2,570654688	0,96528
0,132878587	1,99993	56857,4	3,94948	2,56362054	0,876545
0,108422646	2,00008	56857,4	3,94925	2,56651462	0,96488
0,10565742	1,99998	56857,4	3,94928	2,566160067	0,9761

Table B.3: Data for $4s < \hat{\sigma_T} < 5s$

p-value	$\hat{n_s}$	$\hat{T_0}(MJD)$	γ	$\hat{\sigma_T}$(s)	$-\log_{10} p$
0,095014525	1,99998	56665,2	3,9497	4,492455072	1,02221
0,077753509	1,99998	56665,2	3,94916	4,485219922	1,10928
0,104195749	1,99998	56665,2	3,9493	4,481090783	0,98215
0,04313055	2	56665,2	3,94911	4,466977269	1,365215
0,035212349	2	56665,2	3,94901	4,463378761	1,453305
0,090798777	1,99998	56665,2	3,94974	4,493282689	1,04192
0,037480036	2	56665,2	3,94905	4,464715011	1,4262
0,03059215	2	56665,2	3,94897	4,463481535	1,51439
0,150187919	1,99998	56665,2	3,94966	4,464509408	0,823365
0,062745849	1,99999	56665,2	3,94999	4,472123028	1,202415
0,051276102	1,99999	56665,2	3,94912	4,463995442	1,290085
0,082957375	1,99998	56665,2	3,94997	4,46522906	1,081145
0,268738569	1,99998	56665,2	3,94964	4,470166942	0,57067
0,16157159	1,99998	56665,2	3,94936	4,46522906	0,791635

Bibliography

[1] I. Collaboration. Observation of astrophysical neutrinos in four years of icecube data. *Proceedings of science*, (2015).

[2] I. Collaboration. All-sky search for time-integrated neutrino emission from astrophysical sources with 7 yr of icecube data. *The American Astronomical Society*, (2017).

[3] V. P. EDGAR BUGAEV, PETER KLIMAI. Photon spectra from final stages of a primordial black hole evaporation in different theoretical models. *Proc. of the 30th International Cosmic Ray Conference; R. Caballero et al (eds.); Universidad Nacional Autonoma de Mexico, Mexico City, Mexico, 2008; Vol. 3 (OG part 2), pages 1123-1126*, (2007).

[4] J. L. S. et al. Observational and theoretical aspects of relativistic astrophysics and cosmology. *Singapore : World Scientific*, (1985).

[5] B. K. F. Halze and E. Zas. Neutrino from primordial black holes. *arXiv:hep-ph/9502268v1*, (1995).

[6] J. H. M. . T. C. W. F. Halzen, E. Zas. Gamma rays and energetic particles from primordial black holes. *Nature volume 353, pages 807–815*, (1991).

[7] S. Hawking. Particle creation by black holes. *in Commun.Math.Phys. 43,199-220*, (1975).

[8] S. Hawking. Black holes from cosmic strings. *Physics Letters B231,237*, (1989).

[9] K.K. photomultiplier tube basics and applications. *Hamamatsu Photonics*, (2007).

[10] J. A. A. e. a. M. G. Aertsen, M. Ackermann. Searches for Time Dependent Neutrino Sources with Icecube (Data from 2008 to 2012). *[astro-ph.HE], arXiv:1503.00598v2*, (2015).

[11] e. a. The IceCube Collaboration: R. Abbasi. Time-integrated searches for point-like sources of neutrinos with the 40-string icecube detector. *Astrophys.J.732:18*, (2011).

[12] I. D. Zel'dovich, Ya. B.; Novikov. The hypothesis of cores retarded during expansion and the hot cosmological model. *Astronomicheskii Zhurnal, Vol. 43, p.758*, (1966).